

Temperature dependence of Doppler-broadening in rubidium: An undergraduate experiment

Chris Leahy, J. Todd Hastings, and P. M. Wilt

Citation: *American Journal of Physics* **65**, 367 (1997);

View online: <https://doi.org/10.1119/1.18553>

View Table of Contents: <http://aapt.scitation.org/toc/ajp/65/5>

Published by the American Association of Physics Teachers

Articles you may be interested in

[A narrow-band tunable diode laser system with grating feedback, and a saturated absorption spectrometer for Cs and Rb](#)

American Journal of Physics **60**, 1098 (1998); 10.1119/1.16955

[Doppler-free saturated absorption: Laser spectroscopy](#)

American Journal of Physics **64**, 1432 (1998); 10.1119/1.18457

[Collimated blue light generation in rubidium vapor](#)

American Journal of Physics **81**, 442 (2013); 10.1119/1.4795311

[Wavelengths, Transition Probabilities, and Energy Levels for the Spectra of Rubidium \(RbI through RbXXXVII\)](#)

Journal of Physical and Chemical Reference Data **35**, 301 (2006); 10.1063/1.2035727

[A basic lock-in amplifier experiment for the undergraduate laboratory](#)

American Journal of Physics **71**, 1208 (2003); 10.1119/1.1579497

[Littrow configuration tunable external cavity diode laser with fixed direction output beam](#)

Review of Scientific Instruments **72**, 4477 (2001); 10.1063/1.1419217



American Association of **Physics Teachers**

Explore the **AAPT Career Center** –
access hundreds of physics education and
other STEM teaching jobs at two-year and
four-year colleges and universities.

<http://jobs.aapt.org>



Temperature dependence of Doppler-broadening in rubidium: An undergraduate experiment

Chris Leahy,^{a)} J. Todd Hastings, and P. M. Wilt
Department of Physics, Centre College, Danville, Kentucky 40422

(Received 4 March 1996; accepted 17 September 1996)

This paper describes experiments performed by undergraduate physics majors to measure the temperature dependence of Doppler-broadening in Rb absorption lines over the interval 290–500 K. We report measurements made with a laser-diode spectrometer on the resolved hyperfine transitions of ^{87}Rb ($5^2S_{1/2}$ $F=1$ to $5^2P_{1/2}$, $F=1$ and 2) near 795 nm, and on the unresolved envelope of the transitions of ^{85}Rb ($5^2S_{1/2}$ $F=2$ to $5^2P_{3/2}$, $F=1$, 2 and 3) near 780 nm. Agreement between measured and predicted linewidths is very good. © 1997 American Association of Physics Teachers.

I. INTRODUCTION

It is well known¹ that random thermal motion of atomic absorbers causes a Doppler-broadened absorption line of Gaussian profile; the full-width at half-maximum (FWHM, measured in frequency units) $\Delta\nu$ is given by

$$\Delta\nu = 2\nu_0(2 \ln 2kT/mc^2)^{1/2}, \quad (1)$$

where ν_0 is the transition frequency, k the Boltzmann constant, T the absolute temperature and mc^2 the rest-energy of the absorber. For the Rb D lines at room temperature, Eq. (1) predicts a FWHM of about 500 MHz. This linewidth can easily be observed using temperature-stabilized laser-diodes whose outputs are tunable and have a FWHM typically of less than 100 MHz. We report below our measurements and analysis of the temperature dependence of the FWHM of several hyperfine absorption transitions in ^{85}Rb ($5^2S_{1/2}$ $F=2$ to $5^2P_{3/2}$, $F=1$, 2 and 3, unresolved) and ^{87}Rb ($5^2S_{1/2}$ $F=1$ to $5^2P_{1/2}$, $F=1$ and 2, resolved). In particular, we find very good agreement between measured linewidths and the expected $T^{1/2}$ temperature dependence.

Section II of this paper discusses laser line shape and absorption line convolution, and tabulates the frequency separations and theoretical relative intensities of the hyperfine transitions. Section III describes the experimental apparatus used for data acquisition, while Sec. IV presents the data analyses used to extract measured linewidths from observations. Section V discusses the results and describes how this experimental technique may be used in an undergraduate physics curriculum.

II. THEORETICAL AND COMPUTATIONAL CONSIDERATIONS

As described below, we conducted our measurements at constant pressure equal to the vapor pressure² of Rb at 296 K, or about 9×10^{-5} Pa. Under these conditions the Lorentzian contribution to the linewidth $\Delta\nu$ due to collision broadening³ and the finite lifetime^{4,5} of the involved energy states is about 10 MHz. Since the Doppler-broadened half-widths encountered in our study are in the range 500–650 MHz, we have absorbed these Lorentzian effects into an effective laser linewidth and assumed that our observed hyperfine transitions have an inherent Gaussian profile whose width is given by Eq. (1).

Our absorption measurements were made by tuning laser-diodes across the absorption line. We used two different lasers whose effective linewidths of 75 and 130 MHz are not

negligible compared to the Doppler width. We have assumed that the laser line shape is Lorentzian and will describe in Sec. IV a check of this assumption. Hence our observed absorption profiles will be Voigt since they result from the convolution of the Gaussian Doppler-broadened hyperfine transition with the Lorentzian laser line shape. We have used Jandel's PEAKFITTM software⁶ as a convenient computational mechanism for analyzing Voigt line shapes with varying Gaussian and Lorentzian components.

For data analyses it is necessary to know the frequency separations and relative intensities of the hyperfine transitions under study. These data are given in Table I. We computed the frequency separations from the A and B coefficients given by Arimondo *et al.*⁷ for the appropriate Rb isotope and hyperfine level. Gibbs and Hull⁸ reported theoretical computations of the necessary relative intensities.

III. EXPERIMENTAL APPARATUS

Our experimental design is derived from the saturated absorption spectrometer described by Brandenberger.⁹ We use slightly modified versions of the laser current and temperature controller described in Ref. 9. Figure 1 shows our optical layout which includes a Fabry–Perot frequency marker (free spectral range of 256.18 MHz) and is similar to Brandenberger's Fig. 2 for Experiment 7, except that we dispense with the pump beam and the second probe beam. The diode lasers are Mitsubishi models ML 4102A (for 795 nm) and ML 4402 (for 780 nm); both operated at an output power of about 4 mW. Typically, the laser intensity at the sample was 3 W/m^2 . The most intense transition studied in this work diminished the laser intensity by less than 3%. Our absorption cell¹⁰ is sealed PyrexTM, 10 cm in length, with a centrally attached sidearm which extends 10.2 cm at right angles before turning down another 8 cm. The cell body is designed to be heated in an oven while the sidearm extends outside and may be kept in a room-temperature water bath. This design allows the pressure in the cell to remain at the vapor pressure of Rb in the sidearm, while the temperature of Rb in the cell body may be elevated by increasing the oven temperature.

Figure 2 is a photograph of an oven we designed and constructed for the study. At the center of the oven are two clamshell refractory elements, each containing five nichrome-wire heating coils wound from #22 wire. The coils are placed so that in the closed configuration they axially surround the Rb cell. The elements are molded from high-temperature cement¹¹ and are anchored with standoff insula-

Table I. Frequency separations and relative intensities of observed Rb hyperfine transitions. Comparison of relative intensity is meaningful only for a single isotope.

Isotope	Transition label	Lower state	Upper state	Relative intensity	Frequency separation (MHz)
^{87}Rb	a	$^2S_{1/2}, F=1$	$^2P_{1/2}, F=1$	1	$\Delta\nu_{ab}=812$
	b	$^2S_{1/2}, F=1$	$^2P_{1/2}, F=2$	5	
^{85}Rb	c	$^2S_{1/2}, F=2$	$^2P_{3/2}, F=1$	27	$\Delta\nu_{cd}=29.3$
	d	$^2S_{1/2}, F=2$	$^2P_{3/2}, F=2$	35	
	e	$^2S_{1/2}, F=2$	$^2P_{3/2}, F=3$	28	$\Delta\nu_{de}=64.3$

tors to an aluminum box which forms the outer surface of the oven. Fiberglass insulation fills the space between the box and elements. Pass-through insulators allow the heating coils to be connected to terminal strips external to the box. When closed, the oven encapsulates the cell except for the sidearm which extends outside. The laser beam can pass through the oven along the cell axis.

Figure 2 shows the opened oven with the cell in place. In operation the cell is cushioned with several turns of a high-temperature tape. We monitor cell temperature with thermocouples (not shown) placed at each end and in the middle of the cell. The cell temperature is uniform to better than 1 K and is varied by controlling heating-coil current with a Variac. We can maintain constant temperatures between room and 700 K with this design.

Optical signal voltages from the two photodetectors (one for the FP frequency marker, one from the probe beam passing through the cell) are recorded as a function of elapsed time following a trigger point as the laser is swept through the absorption transitions. These two signals are displayed on a Hewlett-Packard 54512B digitizing oscilloscope which is interfaced through an HP-IB card to a personal computer. Repeated scans through the absorption region can be averaged; we typically used absorption profiles averaged from 16 or 32 scans. In this manner we obtain two data files which consist of x - y pairs of detector voltage at a certain time following oscilloscope trigger. One file contains the absorption signal while the second records the frequency marker.

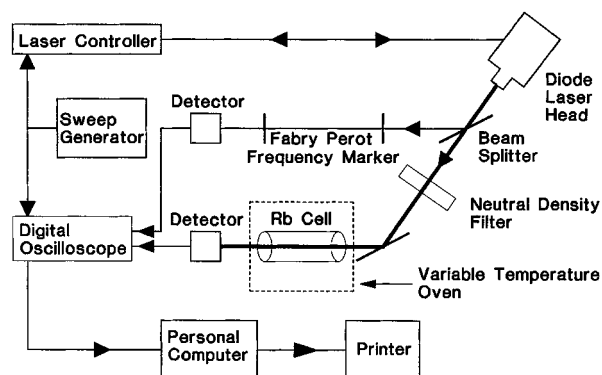


Fig. 1. Experimental block diagram showing optical layout and major components.

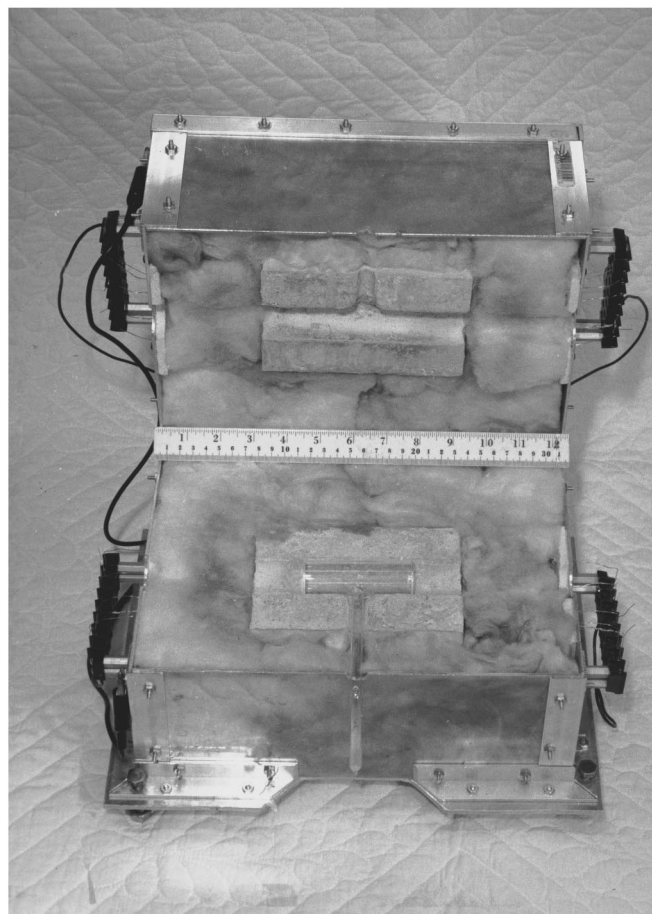


Fig. 2. Photograph of the opened oven and absorption cell used for study of the temperature dependence of Doppler broadening. Note the cell side-arm which extends outside the closed oven. See the text for a full description of the heating elements.

These x - y pairs can each be converted to an intensity-frequency point of an absorption-line spectrum and are in a form accessible as an input file for PEAKFIT.

IV. DATA AND ANALYSIS

A. 795 nm line

In this case we studied the temperature dependence of Doppler-broadening on the resolved ^{87}Rb hyperfine absorption transitions from $F=1$ to $F=1$ and 2. Figure 3 shows the appearance of these transitions at 296, 404, and 500 K. The increase in FWHM with temperature for both transitions is readily apparent.

To analyze these data we must know the line profile for our ML 4102A laser-diode. For this purpose we used partly resolved saturated-absorption¹² data (not shown) for the ^{85}Rb $F=3$ to $F=2$ and 3 hyperfine transitions obtained under identical laser conditions. Assuming that the laser line shape is Lorentzian and using known frequency separations⁷ and relative intensities,⁸ we fit our observed saturated absorption data by varying the FWHM of the laser line. An effective laser linewidth of 130 MHz produced an excellent fit between the simulated and observed spectrum.

We use data taken at 448 K to illustrate our method of analysis. Figure 4(a) shows data as obtained from the storage oscilloscope. The x axis is calibrated in time delay from an

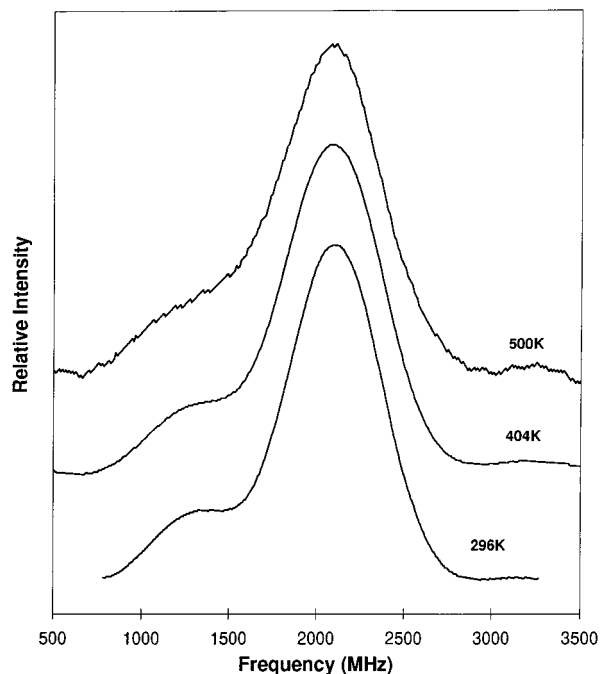
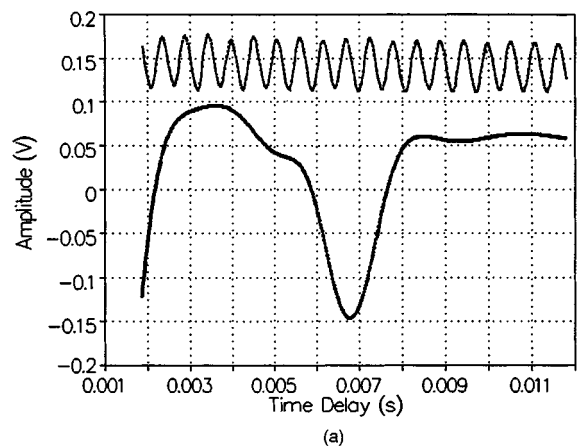


Fig. 3. Traces at three temperatures of the absorption contours of the ^{87}Rb hyperfine components $F=1$ to $F=1$ and 2 near 795 nm. Absorption intensity increases upward on the vertical axis; the horizontal axis records frequency in MHz from an arbitrary zero. Note line broadening with increasing temperature.

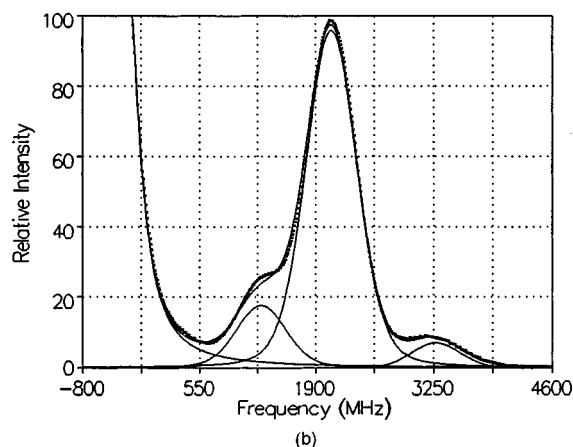
arbitrary trigger point of the frequency sweep, while the y axis gives the signal amplitude for some arbitrary offset. The top curve is the Fabry–Perot frequency-marker signal and the bottom curve is the Rb absorption signal of interest. We use the free-spectral range of the frequency marker to convert the time-delay to a frequency-difference axis. More specifically, we choose the center of a fringe near the beginning of the sweep as time and frequency zero. Next, the time delay of the other peak centers relative to zero is measured. The frequency differences of these peak centers are integral multiples of the free spectral range. We fit these frequency differences to a quadratic in the time delay and thus determined a functional relationship between time delay and frequency difference. The uncertainty in this process is about 10^{-2} fringe, or about ± 2.5 MHz.

To extract the FWHM of the hyperfine components from our data requires a knowledge of their line shapes, frequency separations, and relative intensities. To obtain these from our data requires an accurate knowledge of the baseline and its influence from nearby absorption features; we found it easy to estimate a baseline and vary spectral parameters to obtain an essentially perfect fit to our data. However, the resulting parameters, including FWHM, are correlated and vary with choice of baseline. We thus adopted the following analytical procedure: We made various choices of baseline and allowed PEAKFIT to fit two Voigt lines whose Lorentzian component had a FWHM of 130 MHz to the central two absorption features of Fig. 4(a). Nearby features were also taken into account. We accepted the baseline choice which gave the correct frequency separation and relative intensity for transitions a and b of Table I. PEAKFIT then varied the FWHM of these Voigt lines to obtain the best overall fit for the data.

Figure 4(b) shows the result of the process. The experimental curve has been baseline-subtracted and the y-axis is



(a)



(b)

Fig. 4. (a) Shows observed data at 448 K for the transitions of Fig. 3. The top trace is the Fabry–Perot frequency marker recorded simultaneously with the bottom absorption signal; (b) shows the same data after frequency calibration, inversion, and relative-intensity scaling. Also shown are the fitted Voigt components and their envelope.

inverted and scaled in relative absorption intensity units so that the maximum of transition b equals 100. One can see the excellent fit to the data produced by the two central Voigt components which share the same FWHM and have the correct relative intensities and frequency separations.

We followed this procedure for data taken at ten temperatures in the range 296–500 K. The results are tabulated in Table II and graphed in Fig. 5. The second column of Table II records the theoretical FWHM of a Gaussian Doppler-broadened ^{87}Rb line calculated from Eq. (1) at the indicated temperature. The third column is the FWHM of a Voigt line resulting from the convolution of a 130-MHz Lorentzian laser line with a Gaussian of FWHM given in column 2. We refer to this value as the theoretical FWHM. The fourth column gives the FWHM obtained from our experimental measurements using the analytical procedure described above. Several factors contribute to the experimental uncertainty; we previously mentioned a 2.5 MHz frequency uncertainty. The precision of FWHM measurements on separate signal-averaged spectra obtained at the same temperature is about 2 MHz. The largest uncertainty arises from the range of baselines which will produce acceptable values for the frequency separation and relative intensity of transitions a and b. We find this uncertainty to be about 10 MHz and estimate the total uncertainty of FWHM values to be about ± 10 MHz.

Table II. Comparison between theoretical and measured FWHM for Doppler-broadened ^{87}Rb hyperfine transitions at 795 nm. All values are in MHz. See the text for a full description of the columns.

Temperature (K)	Theoretical FWHM Gaussian component	Theoretical FWHM Voigt line shape	Measured FWHM Voigt line shape
296	502	575	573
325	526	598	592
359	552	625	609
375	565	638	633
404	587	659	658
423	600	672	663
448	618	690	691
473	635	707	705
491	647	719	721
500	653	725	725

B. 780 nm line

Here we studied the temperature dependence of the Doppler-broadened unresolved envelope of the three ^{85}Rb hyperfine transitions $F=2$ to $F=1,2,3$. The analysis was similar to that described for the 795 nm line, was easier because of increased separation from any other nearby overlapping transitions, but was more complicated because of the

Table III. Comparison between theoretical and measured FWHM of Doppler-broadened ^{85}Rb hyperfine transitions at 780 nm. All values are in MHz. See the text for a full description of the columns.

Temperature (K)	Theoretical FWHM Gaussian component	Theoretical FWHM Gaussian envelope	Theoretical FWHM Voigt line shape	Measured FWHM Voigt line shape
294	512	521	562	565
371	575	582	623	640
395	594	600	641	648
434	622	628	669	670
457	638	645	686	681
474	650	656	697	698

unresolved nature of the spectrum. We obtained data at six temperatures in the range of 294–474 K and converted each spectrum to a PEAKFIT file of relative absorption intensity vs frequency. After assuming a Lorentzian shape, we obtained the effective laser linewidth by comparing a resolved saturated absorption spectrum of the ^{87}Rb $F=2$ to $F=1, 2$, and 3 transitions observed with the same ML-4402A laser to a simulation using known relative intensities and frequency separations. The outcome was a laser FWHM of 75 MHz for the operating conditions used for the Doppler study.

The results for these transitions are shown in Table III and Fig. 5. The second column of Table III gives the FWHM of a Gaussian Doppler-broadened hyperfine component for ^{85}Rb at the indicated temperature. Using PEAKFIT, we found that three such overlapping Gaussians of relative intensities and frequencies given for transitions c, d, and e of Table I could be essentially perfectly represented by a Gaussian envelope whose FWHM is given in column 3 of Table III. Surprisingly, the values in the third column are increased by only 6–9 MHz from the second column. The fourth column is the FWHM of a Voigt profile resulting from the convolution of the Gaussian of the third column with the 75 MHz laser linewidth. We call these values the theoretical FWHM. The fifth column records the measured FWHM values which result from fitting a Voigt line shape of 75 MHz Lorentzian component to the experimental envelope of the three unresolved transitions. We again estimate the uncertainty in the measured values to be ± 10 MHz.

V. CONCLUSIONS

As shown in Tables II and III and Fig. 5, our method of analysis, consistently applied, yields very good agreement between theoretical and measured FWHM values for Rb Doppler-broadened hyperfine transitions in the temperature range 294–500 K. Equipment built for saturated absorption spectroscopy, with trivial modification and the addition of an appropriate oven and cell, is capable of producing data accurate enough to illustrate the theoretical dependence of FWHM on the square root of the absolute temperature.

Undergraduate physics majors designed and/or built all equipment used in these experiments with the exception of the absorption cell and the oscilloscope/PC combination. Undergraduates planned the experimental procedures, took the data, contributed to the plan of analysis and analyzed the data for a majority of the temperatures and absorption lines. At each stage of the process there was close collaboration between undergraduates and a faculty mentor. Our experi-

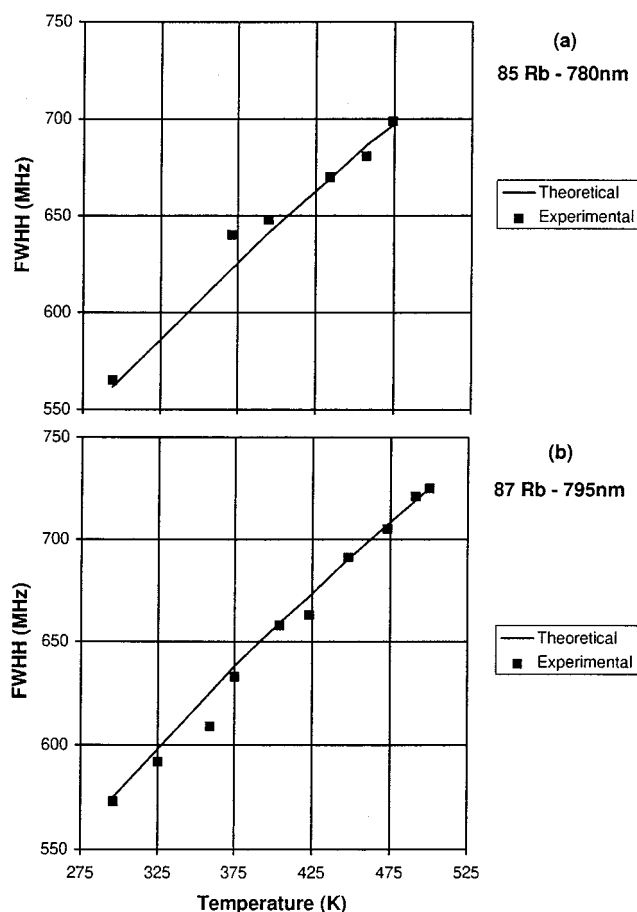


Fig. 5. Plots of the theoretical and experimental FWHM of absorption lines as a function of absolute temperature: (a) is for some ^{85}Rb hyperfine transitions near 780 nm, and (b) for other ^{87}Rb transitions near 795 nm as described in the text.

ence is that this project is an excellent choice for the training of undergraduates with an interest in electronics, optics/quantum optics, and atomic spectroscopy.

This paper reports the results of efforts which extended over four years. Once the equipment was built and tested, actual data acquisition required two weeks. Analysis of data required four months of effort at a pace of perhaps 4 h per week. It is thus clear that such an experiment is too complicated and involved for choice as one of several experiments in an upper-divisional modern physics course. The appropriate utilization of this project in an undergraduate physics curriculum is as a senior project and/or part of an ongoing undergraduate collaborative research project in laser physics and spectroscopy.

ACKNOWLEDGMENTS

We gratefully acknowledge financial support from NSF under ILI Grant No. USE-92-50228 and from the Centre College faculty development committee. Centre undergraduate Paige Anders designed, built, and tested the Fabry–Perot frequency marker, while undergraduate Jeff Pfohl expanded our theoretical understanding of hyperfine splitting in atomic spectroscopy.

^{a)}Present address: Department of Physics, University of Louisville, Louisville, KY 40292.

¹See, for example, Kenneth Krane, *Modern Physics* (Wiley, New York, 1983), pp. 339–340, or A. Corney, *Atomic and Laser Spectroscopy* (Oxford U.P., Oxford, 1977), p. 248.

²A. M. van der Spek, J. J. L. Mulders, and L. W. G. Steenhuysen, “Vapor

Pressure of Rubidium Between 250 and 298 K Determined by Combined Fluorescence and Absorption Measurements,” *J. Opt. Soc. Am. B* **5**, 1478–1483 (1988).

³C. Shang-Yi, “Pressure effects of Homogeneous Rubidium Vapor on its Resonance Lines,” *Phys. Rev.* **58**, 884–887 (1940).

⁴G. P. Barwood *et al.*, “Frequency Measurements on Optically Narrowed Rb-Stabilized Laser Diodes at 780 nm and 795 nm,” *Appl. Phys. B* **53**, 142–147 (1991).

⁵O. S. Heavens, “Radiative Transition Probabilities of the Lower Excited States of Alkali Metals,” *J. Opt. Soc. Am.* **51**, 1058–1061 (1961).

⁶Jandel Scientific Software (San Rafael, CA 94901). This nonlinear curve-fitting software uses the Marquardt–Levenberg algorithm in an iterative process to fit a series of data points with analytical curves of user-defined type and number. See D. W. Marquardt, “An algorithm for least-squares estimation of nonlinear parameters,” *J. Soc. Ind. Appl. Math.* **11**, 431–441 (1963). Sample code for this algorithm is found in Press *et al.*, *Numerical Recipes* (Cambridge U.P., Cambridge, 1986), pp. 523–528.

⁷E. Arimondo, M. Inguscio, and P. Violino, “Experimental Determinations of the Hyperfine Structure in the Alkali Atoms,” *Rev. Mod. Phys.* **49**, 31–75 (1977).

⁸H. M. Gibbs and R. J. Hull, “Spin-Exchange Cross Sections for Rb^{87} – Rb^{87} and Rb^{87} – Cs^{133} Collisions,” *Phys. Rev.* **153**, 132–151 (1967).

⁹J. R. Brandenberger, *Lasers and Modern Optics in Undergraduate Physics* (Lawrence U. P., Appleton, WI, 1989), pp. 43–58.

¹⁰Ophos Instruments, Inc. (Rockville, MD 20855).

¹¹No. 8 Electrotemp Cement, Sauereisen Cements (Pittsburgh, PA 15238-2989). It may be feasible to obtain appropriate heating elements from Watlow (St. Louis, MO 63146).

¹²Reference 9 discusses saturated absorption spectroscopy. Higher resolution may be obtained with an optical feedback system as described by K. B. MacAdam, A. Steinbach, and C. Wieman, “A narrow-band tunable diode laser system with grating feedback, and a saturated absorption spectrometer for Cs and Rb,” *Am. J. Phys.* **60** (12), 1098–1111 (1992).